CONF-850311--1

EFFECT OF TEMPERATURE AND IONIC IMPURITIES AT VERY LOW CONCENTRATIONS ON STRESS CORROSION CRACKING OF TYPE 304 STAINLESS STEEL*

W. E. Ruther, W. K. Soppet, and T. F. Kassner

Materials Science and Technology Division
Argonne National Laboratory
Argonne, Illinois 60439

CONF-850311--1

TI85 003048

November 1984

DISCLAIMER

For presentation at CORROSION/85, Boston, MA, March 25-29, 1985.

*Work supported by the U. S. Nuclear Regulatory Commission, Office of Nuclear Regulatory Research.

EFFECT OF TEMPERATURE AND IONIC IMPURITIES AT VERY LOW CONCENTRATIONS ON STRESS CORROSION CRACKING OF TYPE 304 STAINLESS STEEL

W. E. RUTHER, W. K. SOPPET, and T. F. KASSNER
Materials Science and Technology Division
Argonne National Laboratory
9700 South Cass Avenue
Argonne, Illinois 60439

ABSTRACT

The relative effect of ~12 anion species, in conjunction with hydrogen and sodium cations, on the stress-corrosion-cracking (SCC) behavior of lightly sensitized Type 304 stainless steel was investigated in constant-extension-rate-tensile (CERT) tests at 289°C in water with 0.2 ppm dissolved oxygen at total conductivity values of $\leq$1 μS/cm. The results show that the sulfur species, either in acid or sodium form, produce the highest degree of IGSCC relative to other anions. The effect of temperature on the SCC behavior of the material was investigated in CERT tests over the range 110 to 320°C in high-purity water and in water containing 0.1 and 1.0 ppm sulfate as H_2SO_4 at a dissolved oxygen concentration of 0.2 ppm. The CERT parameters were correlated with impurity concentration (i.e., conductivity) and the electrochemical potential of platinum and Type 304 stainless steel electrodes in the high-temperature environments. Maximum IGSCC occurred at temperatures between ~200 and 250°C in high-purity water, and the addition of sulfate increased the average crack growth rates and the temperature range over which maximum susceptibility occurred. A distinct transition from intergranular to transgranular and ultimately to a ductile failure mode was observed as the temperature increased from ~270 to 320°C in high-purity water. This transition was attributed to a decrease in the open-circuit corrosion potential of the steel below a critical value of ~0 mV(SHE) at the higher temperature. A large decrease in the crack growth rates of fracture-mechanics-type specimens of the steel was also found when the temperature was increased from 289 to 320°C in high-purity water with 0.2 ppm dissolved oxygen.

INTRODUCTION

The role of dissolved oxygen, impurity species, and temperature on intergranular stress corrosion cracking (IGSCC) of sensitized Type 304 stainless steel (SS) is of considerable interest in relation to the numerous

incidents of cracking in recirculation piping of commercial boiling water nuclear reactors (BWRs). In a recent paper,[1] we reported that lightly sensitized Type 304 SS exhibited a particularly high degree of IGSCC susceptibility in CERT tests at 289°C in water containing >0.05 ppm dissolved oxygen and ≲1.0 ppm sulfate as H_2SO_4. At that time, it was not clear whether the phenomenon was peculiar to sulfate or whether other anion species would have a similar effect on the intergranular cracking behavior. Consequently, the relative effect of various anion species at a concentration of 0.1 ppm, in conjunction with hydrogen and sodium cations, on the SCC susceptibility of the same heat of steel in the lightly sensitized condition has been evaluated at 289°C in water containing 0.2 ppm dissolved oxygen. Since none of the anions was found to be more deleterious than sulfate, the effect of temperature on the SCC behavior of the steel was investigated in water containing 0.2 ppm dissolved oxygen and 0, 0.1, and 1.0 ppm sulfate as H_2SO_4. A crack-growth experiment on fracture-mechanics-type specimens was also performed in high-purity water at 289 and 320°C to determine the extent to which the temperature dependence of the CERT parameters (viz., the time-to-failure and average crack growth rate) is reflected in the crack growth behavior under low-frequency, moderate stress intensity, and high load-ratio loading conditions.

EXPERIMENTAL METHODS

The experimental methods for the CERT experiments were described in a previous paper.[1] Briefly, the tests pertaining to the influence of temperature were performed with an Instron Model 1125 tensile testing machine, whereas the experiments with different anions were conducted in a more compliant loading system with a worm gear Jactuator, gear reducer, and variable speed motor loading mechanism. The strain rate of the specimens in the two systems was identical (viz., 1×10^{-6} s^{-1}). Both systems incorporated a small-diameter autoclave and once-through water system. The dissolved oxygen concentration of 0.2 ppm was established by bubbling a 0.5% oxygen-99.5% nitrogen gas mixture through deoxygenated/deionized feedwater (conductance ≲0.2 μS/cm) contained in a 120-L stainless steel tank. Sulfuric acid was added to the feedwater prior to sparging with the gas mixture to insure adequate mixing. A flow rate of ~0.6 L/h was maintained in the autoclave. An external silver chloride (0.1M KCl) reference electrode,[2] a thermocouple, and platinum and Type 304 SS electrodes were located at the outlet of the autoclave to establish the redox and open-circuit corrosion potentials, respectively, at temperatures below 300°C. The measured potentials were converted to the standard hydrogen electrode at each temperature using the thermocell and liquid junction potentials.[3] Commercial instruments were used to monitor the pH, conductivity and dissolved oxygen concentration at the influent and effluent lines of the autoclave. The dissolved oxygen concentration was verified by the colorimetric (CHEMetrics ampules) method.

Cylindrical tensile specimens with a 6.25-mm diameter and 32.0-mm gauge length were machined from stainless steel bar stock, whose composition is given in Table I. The specimen blanks were solution annealed at 1050°C for 0.5 h and water quenched before final machining. The specimens were then sensitized in groups of three or four at 700°C for 0.25 h plus 500°C for 24 h which yielded a degree of sensitization of 2 coulomb/cm^2 by the electrochemical potentiokinetic reactivation (EPR) technique.[4] The specimens were abraded (wet) with 600 grit metallographic paper normal to the gauge length just before insertion into the autoclave. Straining at a rate of 1×10^{-6} s^{-1} was initiated ~20 h after the autoclave reached the test temperature. In general, the potential values from the platinum and stainless steel electrodes changed rapidly during the first several hours after bringing the autoclave to temperature but remained constant over the duration of the CERT test. The autoclave systems were instrumented so that the specimen cooled rapidly after fracture to minimize corrosion of the fracture surfaces. The reduction in area of the

specimens was determined from a low-magnification optical photograph of the fracture surface, taken parallel to the axis of the specimen. The fracture surfaces were evaluated by scanning electron microscopy to determine the fractions of the reduced cross-sectional area with ductile, transgranular, granulated, and intergranular morphologies.[5]

The fracture-mechanics crack growth experiment was performed in a 6-L autoclave equipped with an MTS servo-hydraulic load system. The feedwater was prepared in the same manner as in the CERT tests and the flow rate through the autoclave was ~1.0 L/h. Three 25.4-mm-thick compact tension specimens from the same heat of steel as in the CERT tests were loaded in series. The specimens in the solution-annealed and sensitized conditions (EPR values of 0, 2, and 20 coulomb/cm^2) were fatigue precracked in air at 289°C and tested in high-purity water (~0.15 μS/cm) with 0.2 ppm dissolved oxygen at 289 and 320°C. The specimens were loaded by a positive sawtooth waveform with an initial K_{max} of ~30 MPa•m$^{1/2}$, a load ratio R of 0.95, and a frequency of 8×10^{-2} Hz. The crack lengths were determined during the test by means of compliance measurements obtained from MTS clip gauges mounted on each specimen.

RESULTS

Influence of Anion Species on SCC Susceptibility

The influence of different sodium salts at an anion concentration of 0.1 ppm (total conductivity values of <1 μS/cm) on the CERT parameters of lightly sensitized (EPR = 2 coulomb/cm^2) Type 304 SS specimens in 289°C water containing 0.2 ppm dissolved oxygen is shown in Table II. The results indicate that a ductile plus transgranular failure mode occurred in high-purity water and in water containing nitrate and borate. Only a small decrease in the time to failure resulted from the addition of these ions. The effect of the carbonate and chloride on IGSCC was virtually identical in terms of the various CERT parameters. Phosphate, silicate, and hydroxide appear slightly more detrimental than carbonate and chloride. The sulfur species (viz., sulfate, sulfite, thiosulfate, and sulfide) produced the highest degree of IGSCC in terms of the amount of intergranular cracking and the largest reduction in the time to failure, maximum stress, etc. The relative effect of the various anions on the time-to-failure is shown in Fig. 1. Our results are in reasonable agreement with those obtained on as-welded Type 304 SS specimens (EPR = 0.9 to 3.8 coulomb/cm^2) in 274°C water containing ~0.2 ppm dissolved oxygen and a conductivity of ~1 μS/cm by the addition of Na_2SO_4, Na_2CO_3, NaF, and $NaNO_3$.[6] Nitrate was least deleterious; sulfate and carbonate were equivalent and produced the highest degree of IGSCC in CERT tests[6] at a strain rate of 3.7×10^{-7} s^{-1}. In these experiments, the fracture mode was ductile plus intergranular for the specimens in the different environments including high-purity water with ~0.2 ppm dissolved oxygen.

The effect of the different anions added in acid form on the SCC susceptibility of the steel has also been investigated. The anion concentration was ~0.1 ppm as in the previous experiments and yielded conductivity values of ~1 μS/cm in water with ~0.2 ppm dissolved oxygen. A gas mixture of 0.035% CO_2, 0.54% O_2, and the balance nitrogen was bubbled through deoxygenated feedwater to establish the desired oxygen and carbonate concentrations at 25°C. The other species were added as dilute acids. The results in Table II indicate that the silicate, borate, nitrate, and phosphate produced the smallest reduction in CERT parameters relative to high-purity water; carbonate and chloride were somewhat more deleterious and the sulfur species caused the highest degree of IGSCC. The time to failure of the specimens in the different environments is shown in Fig. 2. The fracture morphology was ductile plus intergranular (i.e., granulated) in these impurity environments.

A comparison of these results with the information in Table II and Fig. 1 for sodium salts indicates that nitrate, borate, carbonate, and

chloride are somewhat more deleterious when added in acid form; however, there is essentially no difference with respect to the sulfur species.

Effect of Temperature on SCC Susceptibility

The effect of temperature over the range of 110 to 320°C on the SCC behavior of lightly sensitized Type 304 SS was investigated in high-purity water and in water containing 0.1 and 1.0 ppm sulfate as H_2SO_4 at a dissolved oxygen concentration of 0.2 ppm. The SCC susceptibility in terms of the various CERT parameters is given in Tables IV to VI for high-purity water and water with 0.1 and 1.0 ppm sulfate as H_2SO_4. The crack growth rates are based on a measurement of the depth of the largest crack in an enlarged micrograph of the fracture surface and the time period from the onset of yield to the point of maximum load on the tensile curve, depicted schematically in Fig. 3. The dependence of the time-to-failure and the crack growth rate on temperature is shown in Figs. 4 and 5, respectively. In terms of the time-to-failure data, the maximum IGSCC susceptibility occurs at temperatures between ~200 and 250°C in high-purity water with ~0.2 ppm dissolved oxygen. The addition of 0.1 ppm sulfate increases both the degree of susceptibility (i.e., decreases the time-to-failure) and the temperature range over which maximum susceptibility occurs. At a sulfate concentration of 1.0 ppm, the IGSCC susceptibility increases markedly at temperatures $\geq$150°C; however, the decrease in susceptibility at temperatures above ~250°C observed in high-purity water does not occur. Relative to high-purity water, sulfate at a concentration of 1 ppm is most deleterious at high temperatures.

The relatively high degree of scatter in the time-to-failure data for the CERT experiments in high-purity water at temperatures between ~170 and 250°C compared to the impurity environments can be attributed to the difference in the number of cracks that initiate at the specimen surface. In the impurity environments, typically three to five thumbnail SCC cracks of approximately equal depth were present on the fracture surface (Fig. 3), whereas in high-purity water only one deep crack was evident in the specimens for which the failure times fall above the curve in Fig. 4. However, a large crack depth coupled with a long failure time (i.e., the time period from yield to the point of maximum load) produced crack-growth-rate values that are consistent with data based on a larger number of cracks, smaller maximum crack depths, and a correspondingly shorter failure times.

The temperature dependence of the crack growth rates in the three environments is shown in Fig. 5. These data also reveal the large effect of sulfate at low concentrations, particularly at temperatures above ~270°C. The broad maximum in the crack growth rate of sensitized Type 304 SS at temperatures between ~200 and 250°C has also been observed in constant load experiments in high-purity water with 40 ppm dissolved oxygen,[7] and in CERT experiments in high-purity water with 0.2[8] and 8 ppm[9] dissolved oxygen and in water containing 8 ppm oxygen and 500 and 1500 ppm boron as H_3BO_3.[9] In the latter experiments, boric acid at relatively high concentrations did not have a deleterious effect on the SCC susceptibility of the steel over the temperature range of 60 to 360°C. At temperatures below ~150°C, boric acid and lithium hydroxide inhibited SCC of sensitized Type 304 SS in aerated water.[9]

A transition from an intergranular to a ductile fracture mode occurred at temperatures above ~270°C and below ~190°C in high-purity water with 0.2 ppm dissolved oxygen. In the impurity environments, ductile failures occurred at temperatures below ~150°C in water with 0.1 and 1.0 ppm sulfate. The transition in the fracture mode (Table IV) from intergranular to transgranular and ultimately to 100% ductile failure in high-purity water with 0.2 ppm dissolved oxygen as the temperature increases from ~270 to 315°C can be explained, in part, by the dependence of the open-circuit corrosion potential of the steel on temperature. The measurements of the steady-state corrosion potential of the steel shown

in Fig. 6 indicate that the potential decreases more rapidly with temperature above ~250°C, and approaches ~0 mV(SHE) at 315°C. Actual measurements of the corrosion potential at this temperature were not possible because of failure of the reference electrode due to softening of the teflon tubing and loss of the electrolyte solution. If the SCC behavior at 315°C is similar to that at 289°C, as shown in Fig. 7,[10] a relatively small decrease in the potential [i.e., from +100 to ~0 mV(SHE)] at a conductivity of ~0.1 μS/cm produces a transition from intergranular to predominately ductile plus transgranular fracture. A similar transition in failure mode at a potential of ~0 mV(SHE) will not occur for conductivity values of 0.9 and 8.0 μS/cm, since the potentials would have to drop below -475 and -560 mV(SHE), respectively. As indicated in Tables V and VI, the fracture morphologies of the specimens at 315°C reveal a large degree of intergranular cracking in the impurity environments.

Influence of Temperature on Crack Growth under Cyclic Loading

A crack growth experiment with fracture-mechanics-type specimens was performed to determine whether the precipitous decrease in crack growth rates and the change in fracture mode of the CERT specimens with increasing temperature was an artifact of the CERT test, i.e., strongly dependent on strain and strain rate as well as the environment. Three compact tension specimens in the solution-annealed and sensitized conditions (EPR values of 0, 2, and 20 coulomb/cm^2) were fatigue precracked in air at 289°C at a low stress intensity and then subjected to cyclic loading with a positive sawtooth waveform at an initial K_{max} of ~30 MPa·m$^{1/2}$, an R value of 0.95, and a frequency of 8 x 10^{-2} Hz in high-purity water with 0.2 ppm dissolved oxygen at 289°C. Steady-state crack growth was established in the three specimens over a period of ~1400 h as shown in Fig. 8. At the end of this period, the temperature of the autoclave was raised from 289 to 320°C with the same feedwater chemistry (i.e., 0.2 ppm dissolved oxygen, 0.15 μS/cm conductance), and compliance measurements were made at ~200-h intervals as before. It is clear that crack growth in the sensitized specimens virtually ceased over the subsequent 1400-h period at 320°C. The measured effluent dissolved oxygen concentration was ~0.2 ppm during the entire experiment. In the last phase of the experiment, the temperature of the autoclave was decreased to 289°C under the same water chemistry and load conditions, and crack growth appears to have resumed in the three specimens at the previous rates. Thus, the crack growth experiment corroborates the strong influence in temperature on SCC behavior of the steel in high-purity water established in the CERT tests.

DISCUSSION

Influence of Anion Impurities

It is clear from the present results that various anion species at low concentrations (corresponding to conductivity values of $\lesssim$1 μS/cm) differ considerably in their effect on the IGSCC behavior of the steel. Consequently, it is unlikely that the cracking behavior of sensitized austenitic stainless steels can be correlated with the conductivity and pH without specific knowledge of the various ions present. In the case of reactor coolant systems, the standard instrumentation used for analyses of the coolant water is, in general, not adequate to determine the concentration of sulfur species that are particularly deleterious from the standpoint of IGSCC even though sulfate is likely to be present in the water at low concentrations ($\lesssim$0.1 ppm) from normal resin leakage from the demineralizer system and from resin regeneration and replacement operations.

Effects of Temperature on SCC

In general, the temperature dependence of the crack growth rate of sensitized Type 304 SS observed in CERT tests (this study and Refs. 8 and 9) and in constant-load[7] experiments, resembles the behavior of Stage II (K-independent) crack growth of Fe-18Ni maraging steels in hydrogen,[11-13] AISI 4130 steel in hydrogen[14-16] and distilled water,[16] H-11 steel in

hydrogen,[17] and AISI 4340 steel in hydrogen,[18,19] H_2S[20,21] and water.[19,22,23] In the gaseous environments, the crack growth rates obtained from fracture-mechanics-type specimens exhibit three distinct regions of temperature dependence. In the low-temperature range ($\lesssim$0°C in the case of the maraging and 4130 steels and $\lesssim$60°C in the 4340 and H-11 steels), hydrogen-assisted Stage II crack growth is a thermally activated process and follows an Arrhenius-type relationship [$da/dt \approx \exp(-\Delta H/RT)$]. At somewhat higher temperatures, the rates reach a maximum and then decrease rapidly with further increases in temperature. The latter transition is strongly dependent on the yield strength of the material and the hydrogen pressure, i.e., the temperature at which the material becomes essentially immune to gaseous hydrogen embrittlement, increases with hydrogen pressure and yield strength. The crack growth rates of the maraging steels in hydrogen and the 4340 steel in H_2S decrease precipitously as the temperature increases compared to the behavior of the 4340 and 4130 steels in hydrogen. In the low-temperature region, the fracture mode of the 4340 steel is predominantly intergranular with respect to the prior austenite grain boundaries, and as the temperature increases, the amount of transgranular dimpled separation increases. For this material, the effect of temperature on the fracture surface morphology in H_2S was essentially identical to that in hydrogen.[21] Over the temperature range of ~1 to 90°C in water, the crack growth rate of AISI 4130 steel increases rapidly with temperature[16] and reaches a maximum value at ~70 to 90°C. Data were not obtained at higher temperatures to determine if the crack growth rates decrease as in the case of the gaseous environments.

In these materials, the transition in the fracture mode and the precipitous decrease in the crack growth rate has been attributed to the partitioning or distribution of hydrogen to different microstructural elements in the low-alloy steel, which is a function of temperature and hydrogen pressure.[21] At low temperatures, it is postulated that most of the hydrogen concentrates at the prior austenite boundaries and crack growth is controlled by the supply of hydrogen from the environment, whereas at higher temperatures, more of the hydrogen may go into the martensite lattice. The gas-adsorbate equilibrium may also shift with temperature in a manner which further reduces the availability of hydrogen at the more susceptible sites and elsewhere in the microstructure, and thus contributes to the decrease in crack growth rate at higher temperature.[21]

Ford[24] has recently reviewed various mechanisms for environmentally controlled fracture and has suggested that there are many common interrelated steps or microprocesses involved in crack advance in ductile alloy/aqueous environments either by hydrogen embrittlement or slip dissolution at the crack front. For example, for given conditions of electrode potential, pH, and anion concentration at the crack tip, both mechanisms depend on the rates of liquid diffusion of species to and from the crack tip, passivation, and oxide rupture since these factors affect the charge passed per unit time in the slip-dissolution model and the adatom coverage and subsequent hydrogen permeation in hydrogen embrittlement models. Thus, it is possible that the mechanisms associated with hydrogen embrittlement and slip dissolution at the crack tip operate simultaneously.

However, in the case of sensitized Type 304 SS in high-purity water, it is unlikely that hydrogen plays a dominant role in the crack growth process despite the strong similarity of the temperature dependence with the behavior of maraging and low-alloy steels in hydrogenous environments. The more likely rate controlling step involves the cathodic reaction [e.g., oxygen reduction in high-purity water, $O_2 + 2H_2O + 4e^- = 4(OH)^-$; or the reduction of oxyanions that contain a central atom which has multiple oxidation states, e.g., $As^{+5} \rightarrow As^{+3}$, when the species is present in sufficient concentration]. The dissolved oxygen concentration[25] and the concentration of oxyanions in deoxygenated water[26] have a strong

influence on the open-circuit corrosion potential of the steel. A good correlation of the crack growth rates and the fracture mode with the open-circuit corrosion and redox potentials was obtained in CERT tests performed under feedwater chemistry control. The corrosion and redox potentials associated with IGSCC of the steel in low-conductivity water containing 0.2 ppm dissolved oxygen are considerably higher (more positive) than the potential values associated with the reduction of hydrogen ions (i.e., $2H^{+} + 2e^{-} = H_2$).

A better understanding of the relative contribution of these mechanisms to IGSCC of sensitized Type 304 SS under simulated BWR-water-chemistry conditions may be obtained from investigations of the influence of loading mode (i.e., tension versus torsion) and temperature on crack propagation behavior. Experiments of this type are in progress on sensitized Type 304 SS in oxygenated water containing sulfate and other anions at low concentrations.

ACKNOWLEDGMENTS

D. J. Dorman and R. R. Schlueter provided valuable assistance in assembling the test facilities and conducting the CERT and cyclic crack growth experiments and S. Mihailovich and R. W. Puccetti obtained the SEM micrographs of the fracture surfaces. This work was supported by the Materials Engineering Branch of the U. S. Nuclear Regulatory Commission, Office of Nuclear Regulatory Research.

REFERENCES

1. W. E. Ruther, W. K. Soppet, G. Ayrault, and T. F. Kassner, Corrosion, Vol. 40, No. 10, pp. 518-527 (1984).

2. P. L. Andresen, "Innovations in Experimental Techniques for Testing in High-Temperature Aqueous Environments," General Electric Corporate Research and Development Report 81CRD088, Schenectady, New York, May 1981.

3. D. D. Macdonald, A. C. Scott, and P. Wentrcek, J. Electrochem. Soc., Vol. 126, No. 6, pp. 908-911 (1978).

4. W. L. Clarke et al., "Detection of Sensitization in Stainless Steel Using Electrochemical Techniques," General Electric Company Report GEAP-21382, August 1976.

5. H. D. Solomon, Corrosion, Vol. 40, No. 9, pp. 493-506 (1984).

6. R. B. Davis and M. E. Indig, "The Effect of Aqueous Impurities on the Stress Corrosion Cracking of Austenitic Stainless Steels in High-Temperature Water," Corrosion 83, Anaheim, CA, April 1983, National Association of Corrosion Engineers, Paper Number 128.

7. N. Ohnaka, S. Syoji, A. Minato, and K. Tanno, "Environmental Effects on the Intergranular Stress Corrosion Cracking Susceptibility of Sensitized Type 304 Stainless steel in High-Temperature Water," in Predictive Methods for Assessing Corrosion Damage to BWR Piping and PWR Steam Generators, NACE, H. Okada and R. Staehle, eds., pp. 90-92, 1978.

8. F. P. Ford and M. J. Povich, Corrosion, Vol. 35, No. 12, pp. 569-574 (1979).

9. K. Arioka, M. Hourai, S. Okamoto, and K. Onimura, "The Effects of Boric Acid, Solution Temperature, and Sensitization on the SCC Behavior under Elevated Temperature Water," Corrosion 83, Anaheim, CA, April 18-22, 1983, Paper Number 135.

10. W. E. Ruther, W. K. Soppet, and T. F. Kassner, in "Materials Science and Technology Division Light-Water Reactor Safety Research Program: Quarterly Progress Report," April-June 1983, NUREG/CR-3689 Vol. II, ANL-83-85 Vol. II (June 1984), pp. 31-60.

11. S. J. Hudak and R. P. Wei, Met. Trans., Vol. 7A, pp. 235-241 (1976).

12. P. S. Pao and R. P. Wei, Scripta Met., Vol. 11, pp. 515-520 (1977).

13. R. P. Gangloff and R. P. Wei, Met. Trans., Vol. 8A, pp. 1043-1053 (1977).

14. D. P. Williams and H. G. Nelson, Met. Trans., Vol. 1, pp. 63-68 (1970).

15. H. G. Nelson, D. P. Williams, and A. S. Tetelman, Met. Trans., Vol. 2, pp. 953-959 (1971).

16. H. G. Nelson and D. P. Williams, "Quantitative Observations of Hydrogen-induced Slow Crack Growth in a Low Alloy Steel," in Stress Corrosion Cracking and Hydrogen Embrittlement of Iron-base Alloys, J. Hochmann, J. Slater, and R. W. Staehle, eds., NACE, pp. 390-404 (1978).

17. H. H. Johnson, "Hydrogen Brittleness in Hydrogen and Hydrogen-Oxygen Gas Mixtures," ibid., pp. 382-389 (1978).

18. G. W. Simmons, P. S. Pao, and R. P. Wei, Met. Trans., Vol. 9A, pp. 1147-1158 (1978).

19. M. Lu, P. S. Pao, N. H. Chan, K. Klier, and R. P. Wei, "Hydrogen Assisted Crack Growth in AISI 4340 Steel," in Hydrogen in Metals, Supplement to Trans. of the Japan Inst. of Metals, Vol. 21, pp. 449-452 (1980).

20. M. Lu, P. S. Pao, T. W. Weir, G. W. Simmons, and R. P. Wei, Met. Trans., Vol. 12A, pp. 805-811 (1981).

21. M. Gao, M. Lu, and R. P. Wei, Met. Trans., Vol. 15A, pp. 735-746 (1984).

22. W. A. Van Der Sluys, Eng. Fract. Mech., Vol. 1, pp. 447-462 (1969).

23. J. D. Landes and R. P. Wei, Int. Journ. of Fracture, Vol. 9, pp. 277-293 (1973).

24. F. P. Ford, "Stress Corrosion Cracking," in Corrosion Processes, R. N. Parkins, ed., Applied Science Publishers, New York, pp. 271-309 (1982).

25. W. E. Ruther, W. K. Soppet, and T. F. Kassner, in "Materials Science and Technology Division Light-Water Reactor Safety Research Program: Quarterly Progress Report," October-December 1983, NUREG/CR-3689 Vol. IV, ANL 83-85 Vol. IV, pp. 51-91, August 1984.

26. W. E. Ruther, W. K. Soppet, and T. F. Kassner, to be published in "Light-Water Reactor Safety Materials Engineering Research Program: Quarterly Progress Report," October-December 1984, NUREG/CR-3998 Vol. IV, ANL-84-60 Vol. IV, 1985.

TABLE I. Composition of AISI 304 SS (Heat No. 30956) in wt %

Cr	Ni	Mn	Si	Mo	Cu	Co	N	C	P	S	Fe
18.99	8.00	1.54	0.48	0.44	0.19	0.10	0.10	0.06	0.019	0.007	Balance

TABLE II. Influence of Different Anions at Concentration[a] of 0.1 ppm on the SCC Susceptibility of Sensitized (EPR = 2 C/cm^2) Type 304 SS Specimens[b] (Heat No. 30956) in 289°C Water Containing 0.2 ppm Dissolved Oxygen

Test No.	Feedwater Chemistry				CERT Parameters				
	Oxygen, ppm	Impurity Species	Cond. at 25°C, µS/cm	pH at 25°C	Failure Time, h	Maximum Stress, MPa	Total Elong., %	Reduction in Area, %	Fracture Morphology[c]
A2	0.24	-	0.14	6.12	166	493	60	66	0.80D, 0.20T
A50	0.24	$NaNO_3$	0.34	6.03	152	516	55	60	0.85D, 0.15T
A51	0.26	$Na_2B_4O_7$	0.21	6.40	142	523	51	68	0.88D, 0.12T
A48	0.30	Na_2CO_3	0.43	6.80	103	476	37	43	0.60D, 0.40G_3
A49	0.31	NaCl	0.51	6.05	98	476	35	50	0.58D, 0.42G_2
A65	0.22	Na_3PO_4	0.47	6.93	84	448	30	30	0.57D, 0.43G_3
A66	0.25	Na_2HPO_4	0.33	6.47	84	425	30	54	0.29D, 0.71G_3
A47	0.25	Na_2SiO_3	0.53	7.62	69	398	25	43	0.55D, 0.45I
A71	0.21	NaOH	1.16	8.34	68	390	24	52	0.22D, 0.34T, 0.44G_3
A12	0.20	Na_2SO_4	0.66	6.90	54	345	20	29	0.22D, 0.78G_3
A53	0.26	Na_2SO_3	0.36	6.44	47	329	17	22	0.22D, 0.78I
A52	0.23	$Na_2S_2O_3$	0.47	6.15	49	299	18	14	0.12D, 0.88G_3
A54	0.22	Na_2S	1.03	8.05	49	317	18	23	0.22D, 0.78G_3

[a]Anion concentration of 0.1 ppm is based on complete dissociation of the amount of the salt added to the feedwater without consideration of the actual dissociation equilibria at 25 or 289°C.
[b]Specimens were exposed to the environment for ~20 h at 289°C before straining at a rate of 1×10^{-6} s^{-1}.
[c]Ductile (D), transgranular (T), granulated (G), intergranular (I), in terms of the fraction of the reduced cross-sectional area. Characterization of the fracture surface morphologies is in accordance with the illustrations and definitions provided in Ref. 5.

TABLE III. Influence of Different Acids at an Anion Concentration[a] of 0.1 ppm on the SCC Susceptibility of Sensitized (EPR = 2 C/cm^2) Type 304 SS Specimens[b] (Heat No. 30956) in 289°C Water Containing 0.2 ppm Dissolved Oxygen

	Feedwater Chemistry				CERT Parameters				
Test No.	Oxygen, ppm	Impurity Species	Cond. at 25°C, µS/cm	pH at 25°C	Failure Time, h	Maximum Stress, MPa	Total Elong., %	Reduction in Area, %	Fracture Morphology[c]
A2	0.24	-	0.14	6.12	166	493	60	66	0.80D, 0.20T
A59	0.18	H_2SiO_3	0.12	6.25	123	514	44	48	0.63D, 0.37G_3
A57	0.23	H_3BO_3	0.14	6.30	109	492	39	41	0.59D, 0.41G_3
A56	0.24	HNO_3	0.70	5.75	101	481	36	41	0.69D, 0.31G_3
A64	0.23	H_3PO_4	0.53	5.90	99	460	36	53	0.44D, 0.56G_3
A60	0.22	H_2CO_3	0.69	5.77	91	469	33	38	0.52D, 0.48G_2
A58	0.26	HCl	1.19	5.58	83	440	30	37	0.43D, 0.57G_2
A3	0.20	H_2SO_4	0.91	5.74	79	402	29	37	0.22D, 0.78G_2
A63	0.23	H_2SO_4	0.94	5.75	54	326	19	18	0.25D, 0.75I
A61	0.21	H_2SO_3	0.61	5.78	51	320	18	20	0.22D, 0.78G_3

[a]Anion concentration of 0.1 ppm is based on complete dissociation of the amount of acid added to the feedwater without consideration of actual dissociation equilibria at 25 or 289°C.
[b]Specimens were exposed to the environment for ~20 h at 289°C before straining at a rate of 1 x 10^{-6} s^{-1}.
[c]Ductile (D), transgranular (T), granulated (G), and intergranular (I) in terms of the fraction of the reduced cross-sectional area. Characterization of the fracture surface morphologies is in accordance with the illustrations and definitions provided in Ref. 5.

TABLE IV. Effect of Temperature on the SCC Susceptibility and Crack Growth Rate of Lightly Sensitized (EPR = 2 C/cm^2) Type 304 SS Specimens[a] (Heat No. 30956) from CERT Experiments in Water Containing 0.2 ppm Dissolved Oxygen

		Feedwater Chemistry										
Test No.	Temp., °C	Oxygen, ppm	Sulfate, ppm	Cond., µS/cm	pH at 25°C	Failure Time, h	Maximum Stress, MPa	Total Elong., %	Reduction in Area, %	Fracture Morphology[b]	SCC Growth Rate,[c] mm·h^{-1}	m·s^{-1}
123	320	0.17	0	0.11	6.28	156	534	56	72	1.00D	0	0
96	315	0.21	0	0.13	6.19	151	538	55	75	1.00D	0	0
122	300	0.18	0	0.19	6.18	154	538	55	76	0.97D, 0.03T	1.9 x 10^{-3}	5.3 x 10^{-10}
2	289	0.25	0	0.20	6.80	143	492	50	52	0.69D, 0.31T	7.9 x 10^{-3}	2.2 x 10^{-9}
94	270	0.24	0	0.12	6.08	123	513	44	49	0.43D, 0.57G_3	1.4 x 10^{-2}	3.9 x 10^{-9}
98	250	0.22	0	0.10	6.21	115	499	41	46	0.28D, 0.72G_3	1.3 x 10^{-2}	3.6 x 10^{-9}
91	240	0.24	0	0.10	6.15	71	328	25	31	0.40D, 0.60I	3.3 x 10^{-2}	9.2 x 10^{-9}
95	225	0.23	0	0.12	6.15	105	448	40	64	0.41D, 0.59I	1.7 x 10^{-2}	4.7 x 10^{-9}
97	225	0.21	0	0.11	6.19	80	448	29	33	0.50D, 0.50I	2.2 x 10^{-2}	6.1 x 10^{-9}
125	215	0.21	0	0.14	6.17	132	516	48	72	0.80D, 0.20I	1.4 x 10^{-2}	3.9 x 10^{-9}
119	205	0.23	0	0.14	6.26	98	456	35	66	0.67D, 0.33G_3	1.9 x 10^{-2}	5.2 x 10^{-9}
92	190	0.24	0	0.13	6.07	96	449	34	62	0.67D, 0.33I	2.3 x 10^{-2}	6.4 x 10^{-9}
124	175	0.22	0	0.14	6.23	157	509	57	80	1.00D	0	0
120	165	0.21	0	0.15	6.24	151	502	54	80	0.79D, 0.21T	7.2 x 10^{-3}	2.0 x 10^{-9}
121	150	0.19	0	0.13	6.24	148	491	53	80	0.99D, 0.01T	1.7 x 10^{-3}	4.7 x 10^{-10}
93	140	0.22	0	0.12	6.10	155	514	56	81	1.00D	0	0
99	110	0.20	0	0.12	6.20	173	523	62	84	1.00D	0	0

[a]Specimens were exposed to the environment for ~20 h before straining at a rate of 1 x 10^{-6} s^{-1}.
[b]Ductile (D), transgranular (T), granulated (G), intergranular (I), in terms of the fraction of the reduced cross-sectional area. Characterization of the fracture surface morphologies is in accordance with the illustrations and definitions provided in Ref. 5.
[c]SCC growth rates are based on measurement of the depth of the largest crack in an enlarged micrograph of the fracture surface and the time period from the onset of yield to the point of maximum load on the tensile curve.

TABLE V. Effect of Temperature on the SCC Susceptibility and Crack Growth Rate of Lightly Sensitized (EPR = 2 C/cm^2) Type 304 SS Specimens[a] (Heat No. 30956) from CERT Experiments in Water Containing 0.2 ppm Dissolved Oxygen and 0.1 ppm Sulfate as H_2SO_4

Test No.	Temp., °C	Feedwater Chemistry: Oxygen, ppm	Sulfate, ppm	Cond., µS/cm	pH at 25°C	Failure Time, h	Maximum Stress, MPa	Total Elong., %	Reduction in Area, %	Fracture Morphology[b]	SCC Growth Rate,[c] mm·h^{-1}	m·s^{-1}
116	315	0.20	0.1	0.89	5.70	98	477	35	41	0.44D, 0.28T, 0.28I	3.0×10^{-2}	8.3×10^{-9}
100	315	0.22	0.1	0.87	5.71	87	435	31	48	0.33D, 0.44T, 0.23I	2.3×10^{-2}	6.4×10^{-9}
118	300	0.19	0.1	0.91	5.75	56	382	20	20	0.32D, 0.68I	4.1×10^{-2}	1.1×10^{-8}
17	289	0.18	0.1	0.90	5.80	49	315	18	10	0.08D, 0.92I	8.2×10^{-2}	2.3×10^{-8}
115	289	0.22	0.1	0.90	5.76	62	372	22	21	0.22D, 0.78G_3	3.2×10^{-2}	8.9×10^{-9}
101	270	0.22	0.1	0.87	5.75	61	324	22	21	0.21D, 0.79I	3.9×10^{-2}	1.1×10^{-8}
104	255	0.20	0.1	0.90	5.78	61	358	22	30	0.25D, 0.75I	3.9×10^{-2}	1.1×10^{-8}
102	240	0.22	0.1	0.87	5.73	56	339	20	19	0.35D, 0.65I	4.0×10^{-2}	1.1×10^{-8}
103	225	0.22	0.1	0.88	5.76	50	317	18	26	0.28D, 0.72I	6.0×10^{-2}	1.7×10^{-8}
105	190	0.23	0.1	0.86	5.68	53	340	19	24	0.31D, 0.69I	4.4×10^{-2}	1.2×10^{-8}
106	165	0.19	0.1	0.86	5.71	81	434	29	46	0.44D, 0.56I	3.1×10^{-2}	8.6×10^{-9}
117	150	0.20	0.1	0.88	5.77	84	405	30	27	0.36D, 0.64I	2.7×10^{-2}	7.5×10^{-9}
107	140	0.22	0.1	0.87	5.75	163	504	59	81	1.00D	0	0

[a]Specimens were exposed to the environment for ~20 h before straining at a rate of 1×10^{-6} s^{-1}.
[b]Ductile (D), transgranular (T), granulated (G), intergranular (I), in terms of the fraction of the reduced cross-sectional area. Characterization of the fracture surface morphologies is in accordance with the illustrations and definitions provided in Ref. 5.
[c]SCC growth rates are based on measurement of the depth of the largest crack in an enlarged micrograph of the fracture surface and the time period from the onset of yield to the point of maximum load on the tensile curve.

TABLE VI. Effect of Temperature on the SCC Susceptibility and Crack Growth Rate of Lightly Sensitized (EPR = 2 C/cm^2) Type 304 SS Specimens[a] (Heat No. 30956) from CERT Experiments in Water Containing 0.2 ppm Dissolved Oxygen and 1.0 ppm Sulfate as H_2SO_4

Test No.	Temp., °C	Feedwater Chemistry: Oxygen, ppm	Sulfate, ppm	Cond., µS/cm	pH at 25°C	Failure Time, h	Maximum Stress, MPa	Total Elong., %	Reduction in Area, %	Fracture Morphology[b]	SCC Growth Rate,[c] mm·h^{-1}	m·s^{-1}
108	315	0.22	1.0	8.0	4.78	42	264	15	16	0.14D, 0.86G_3	7.1×10^{-2}	2.0×10^{-8}
39	289	0.20	1.0	8.0	4.80	45	291	16	15	0.19D, 0.81I	9.6×10^{-2}	2.4×10^{-8}
19	289	0.20	1.0	9.0	4.80	40	277	14	11	0.06D, 0.94I	1.1×10^{-1}	3.1×10^{-8}
109	270	0.23	1.0	8.3	4.77	44	291	16	19	0.22D, 0.78I	5.3×10^{-2}	1.5×10^{-8}
110	240	0.23	1.0	8.2	4.77	56	336	20	23	0.14D, 0.86I	5.6×10^{-2}	1.6×10^{-8}
114	215	0.27	1.0	8.0	4.77	50	307	18	15	0.14D, 0.86I	8.1×10^{-2}	2.3×10^{-8}
111	190	0.25	1.0	8.1	4.77	59	359	21	18	0.15D, 0.85I	6.2×10^{-2}	1.7×10^{-8}
113	165	0.26	1.0	8.2	4.78	63	395	23	17	0.05D, 0.95I	5.0×10^{-2}	1.4×10^{-8}
112	140	0.21	1.0	8.2	4.78	156	506	56	-	-	-	-

[a]Specimens were exposed to the environment for ~20 h before straining at a rate of 1×10^{-6} s^{-1}.
[b]Ductile (D), transgranular (T), granulated (G), intergranular (I), in terms of the fraction of the reduced cross-sectional area. Characterization of the fracture surface morphologies is in accordance with the illustrations and definitions provided in Ref. 5.
[c]SCC growth rates are based on measurement of the depth of the largest crack in an enlarged micrograph of the fracture surface and the time period from the onset of yield to the point of maximum load on the tensile curve.

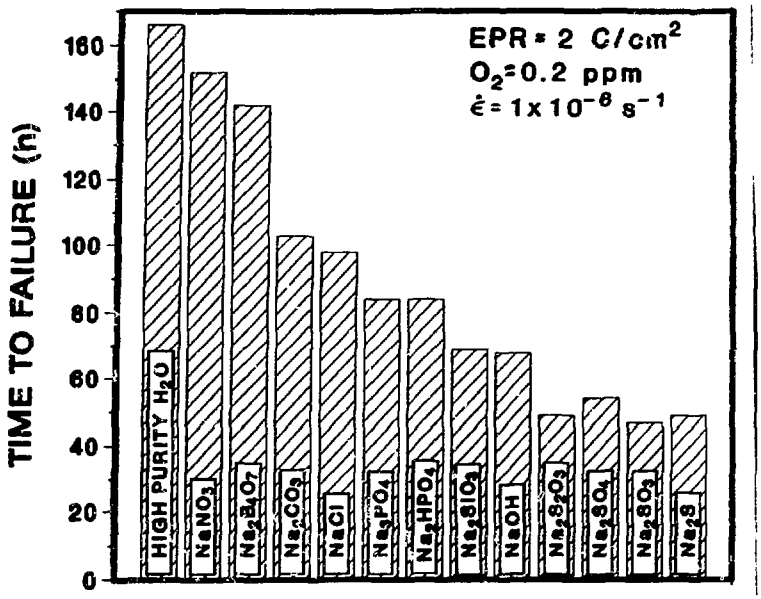

FIGURE 1 - Effect of Various Sodium Salts at an Anion Concentration of 0.1 ppm in Water Containing 0.2 ppm Dissolved Oxygen on the Time-to-Failure of Lightly Sensitized Type 304 SS Specimens in CERT Experiments at 289°C and a Strain Rate of 1 x 10^{-6} s^{-1}.

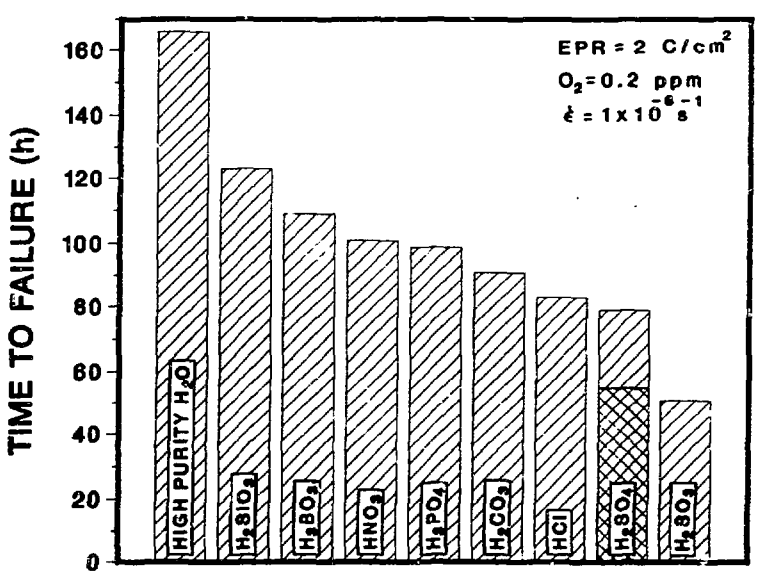

FIGURE 2 - Influence of Various Acids at an Anion Concentration of 0.1 ppm in Water Containing 0.2 ppm Dissolved Oxygen on the Time-to-Failure of Lightly Sensitized (EPR = 2 C/cm^2) Type 304 SS Specimens in CERT Experiments at 289°C and a Strain Rate of 1 x 10^{-6} s^{-1}.

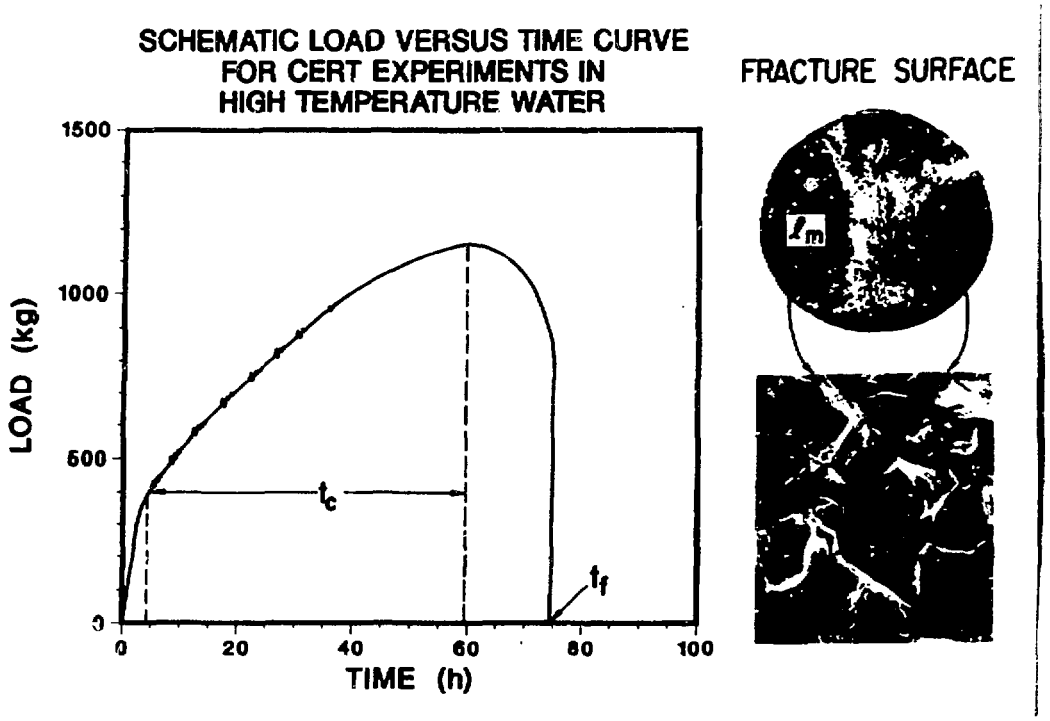

FIGURE 3 - Information from the Load versus Time Curve and the Fracture Surface of CERT Specimens to Determine the SCC Growth Rate.

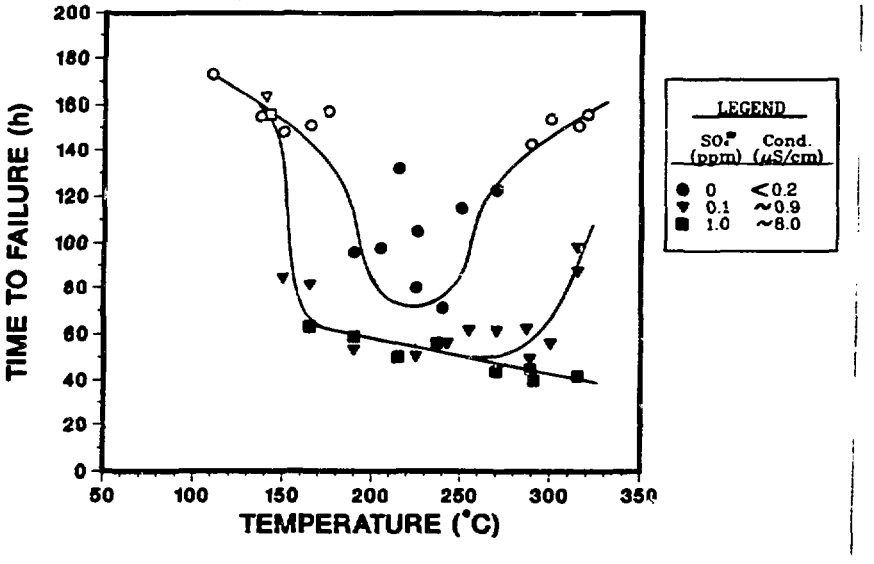

FIGURE 4 - Effect of Temperature on the Time-to-Failure of Lightly Sensitized (EPR = 2 C/cm^2) Type 304 SS Specimens in CERT Experiments at a Strain Rate of 1×10^{-6} s^{-1} in Water Containing 0.2 ppm Dissolved Oxygen and 0, 0.1, and 1 ppm Sulfate as H_2SO_4. Open and closed symbols denote either ductile or ductile plus transgranular and ductile plus intergranular fracture morphology, respectively.

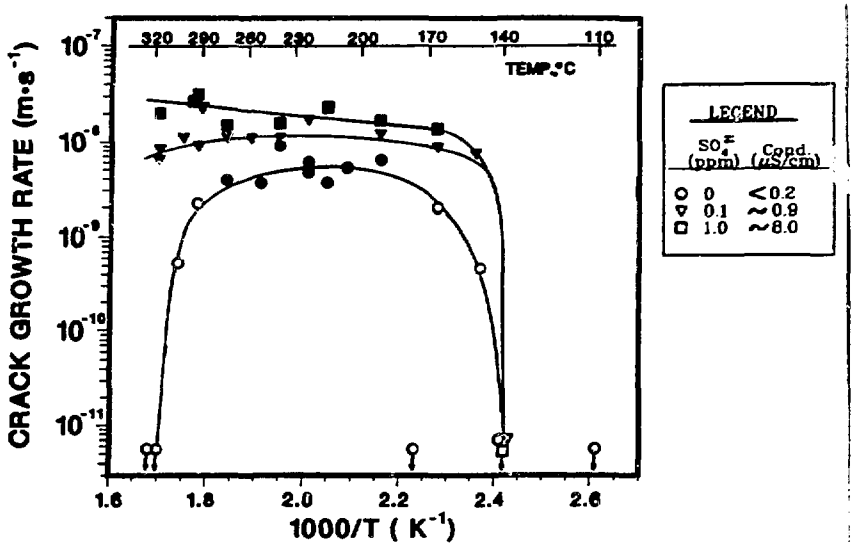

FIGURE 5 - Effect of Temperature on the Crack Growth Rate of Lightly Sensitized (EPR = 2 C/cm^2) Type 304 SS Specimens from CERT Experiments at a Strain Rate of 1 x 10^{-6} s^{-1} in Water Containing 0.2 ppm Dissolved Oxygen and 0, 0.1, and 1 ppm Sulfate as H_2SO_4. Open and closed symbols denote either ductile or ductile plus transgranular and ductile plus intergranular fracture morphology, respectively.

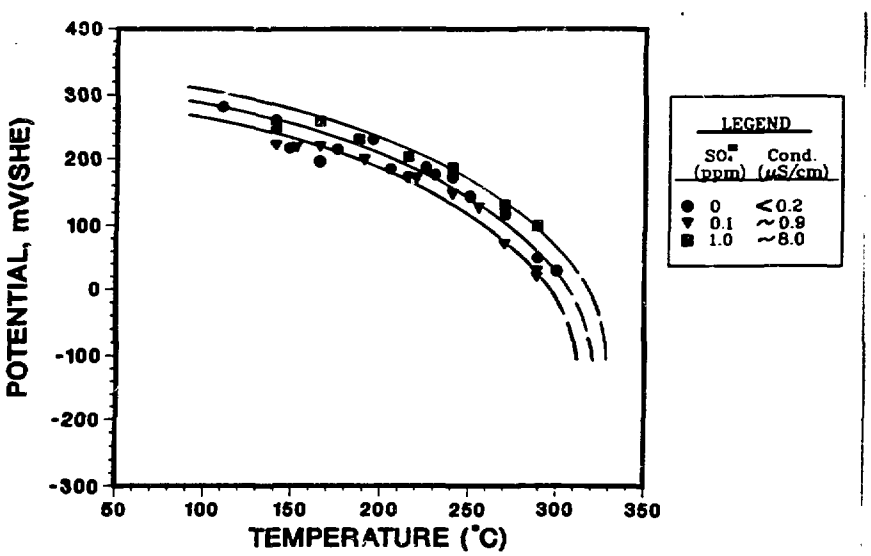

FIGURE 6 - Effect of Temperature on the Electrochemical Potential of Type 304 SS in Water Containing 0.2 ppm Dissolved Oxygen and 0, 0.1, and 1 ppm Sulfate as H_2SO_4.

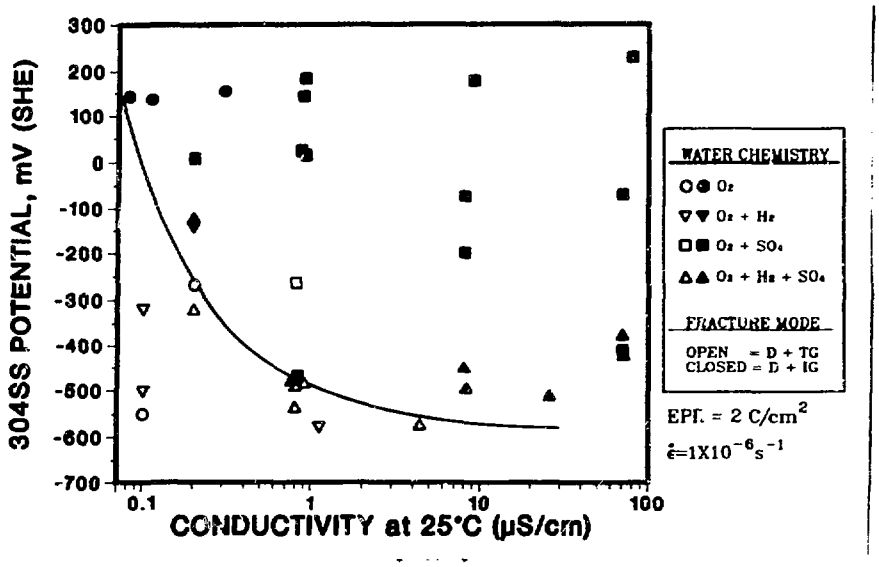

FIGURE 7 - Regime of Corrosion Potential and Feedwater Conductivity that Results in Immunity to IGSCC of Lightly Sensitized (EPR = 2 C/cm^2) Type 304 SS in CERT Experiments at 289°C in Simulated BWR-Quality Water Containing Dissolved Oxygen, Hydrogen, and Sulfate as H_2SO_4.[10]

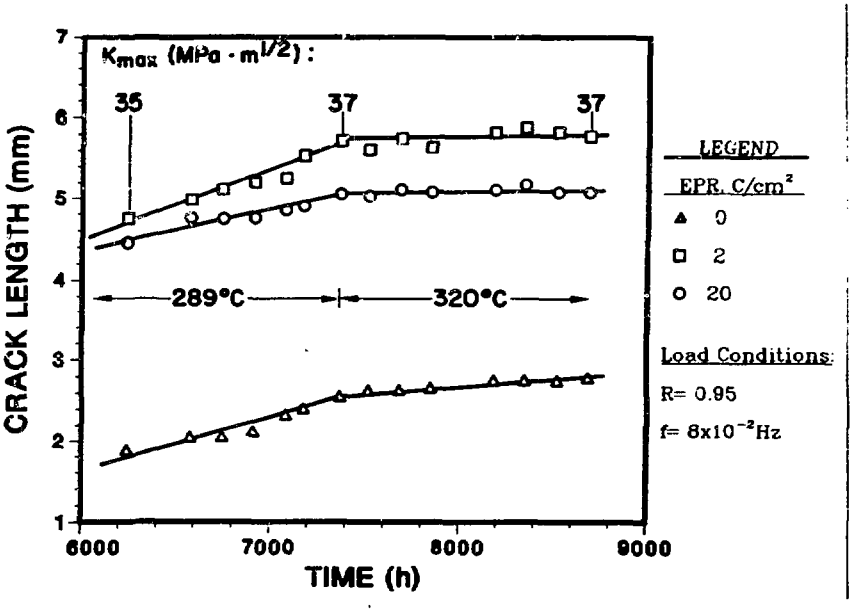

FIGURE 8 - Crack Length versus Time for 1TCT Specimens of Solution-annealed (EPR = 0) and Sensitized (EPR = 2 and 20 C/cm^2) Type 304 SS in High-Purity Water Containing 0.2 ppm Dissolved Oxygen at 289 and 320°C. The loading conditions for the positive sawtooth waveform with a slow loading time (12 s) and rapid unloading (1 s) are as follows: stress ratio R = 0.95, frequency = 8 x 10^{-2} Hz, and K_{max} = 35-37 $MPa \cdot m^{1/2}$ for the specimen with the largest crack.